3-1-2006

Radiative Electron Capture into High- Z Few-Electron Ions: Alignment of the Excited Ionic States

Andrey S. Surzhykov

Ulrich D. Jentschura
Missouri University of Science and Technology, ulj@mst.edu

Th H. Stohlker

Stephan Fritzsche

Recommended Citation

A. S. Surzhykov et al., "Radiative Electron Capture into High- Z Few-Electron Ions: Alignment of the Excited Ionic States," *Physical Review A - Atomic, Molecular, and Optical Physics*, vol. 73, no. 3, pp. 032716-1-032716-8, American Physical Society (APS), Mar 2006.
The definitive version is available at https://doi.org/10.1103/PhysRevA.73.032716

Radiative electron capture into high-Z few-electron ions: Alignment of the excited ionic states

Andrey Surzhykov* and Ulrich D. Jentschura
Max-Planck-Institut für Kernphysik, Saupfercheckweg 1, D-69117 Heidelberg, Germany

Thomas Stöhlker
Gesellschaft für Schwerionenforschung (GSI), D-64291 Darmstadt, Germany and
Institut für Kernphysik, Universität Frankfurt, D-60486 Frankfurt, Germany

Stephan Fritzsche†
Institut für Physik, Universität Kassel, D-34132 Kassel, Germany

(Received 18 November 2005; revised manuscript received 17 January 2006; published 17 March 2006)

We lay out a unified formalism for the description of radiative electron capture into excited states of heavy, few-electron ions and their subsequent decay, including a full account of many-electron effects and higher-order multipoles of the radiation field. In particular, the density-matrix theory is applied to explore the magnetic sublevel population of the residual ions, as described in terms of alignment parameters. For the electron capture into the initially hydrogenlike U^{91+} and lithiumlike U^{89+} uranium projectiles, the alignment parameters are calculated, within the multiconfiguration Dirac-Fock approach, as a function of the collision energy and for different ionic states. From these calculations, we find that the many-electron interactions may result in a small enhancement of the alignment, and that this effect becomes more pronounced for highly excited levels.

DOI: 10.1103/PhysRevA.73.032716 PACS number(s): 34.70.+e, 31.25.−v, 31.30.Jv

I. INTRODUCTION

Collisions of highly charged ions with electronic and atomic targets have been explored intensively in the past both in experiment [1–7] and by theory [8–17]. One of the basic processes in such collisions is the transfer of an electron from the target into a bound state of the projectile ion. For energetic, high-Z ions, this charge transfer is usually accompanied by the simultaneous emission of an x-ray photon which carries away the excess energy and momentum. In fact, the radiative electron capture (REC) of ions, which is equivalent to time-reversed photoionization, is known as a dominant (loss) process for high-energetic ion beams at storage rings. During the last decade therefore a number of experiments have been performed at the GSI storage ring in order to investigate the REC for various elements and for a wide range of projectile energies [2–4]. Most of these studies, however, have been focused on the recombination of (initially) *bare* projectile ions. For such ions, measurements were performed for the total and angle-differential REC cross sections [2], the polarization of emitted x-ray photons, and even the angular distributions of the characteristic Lyman-$\alpha_{1,2}$ radiation [14], if the electron is captured into an excited ionic state. Usually, the experimental findings were found to be in a good agreement with computations, based on the density-matrix approach and the relativistic Dirac's theory [11–13,17,18].

Apart from the REC into *bare* projectiles, less attention was paid previously to the electron capture into *few-electron* ions for which, additionally, electron-electron interaction effects should be taken into account. A first step towards the analysis of such effects was done by Bednarz and co-workers [5], who measured the angle-differential K- and L-shell cross sections for the electron recombination into hydrogen-, helium-, and lithiumlike uranium ions at a single projectile energy of $T_p=216$ MeV/u. For this—rather high—collision energy, however, no signature of electron-electron correlations was observed when the (measured) angular distributions are compared to appropriately scaled one-electron computations. Slightly stronger interelectronic effects were predicted recently by us [19] for less energetic high-Z ions. However, at present-day storage rings, no projectiles are available with energies $T_p \leqslant 1$ MeV/u and hence not much can be learned today about the electron-electron interaction by just studying the total and angle-differential REC cross sections. An alternative way to obtain information on the radiative recombination by few-electron, heavy ions is given by the measurements of the subsequent radiative decay following the electron capture into excited ionic states. Recently, for example, the REC into the $1s2p_{1/2}$ and $1s2p_{3/2}$ $^{1,3}P_J$ levels of (initially) hydrogenlike uranium ions U^{91+} and their subsequent $K\alpha_1$ and $K\alpha_2$ radiative decay have been observed at the GSI storage ring [20,21] and gave rise to an angular distribution, quite in contrast to what is usually expected from the viewpoint of a one-particle model. A more detailed theoretical analysis is therefore required on capture into the excited states of few-electron ions, including a careful treatment of the electron correlations.

In this contribution, we apply the density-matrix formalism from our recent paper [19] to explore a REC process, in which (i) a free (or quasifree) electron is initially captured into the excited state of a high-Z, few-electron ion and which (ii) subsequently decays under the emission of characteristic radiation. Because the properties of this radiation are closely related to the alignment of the excited ionic states, we have

*Electronic address: surz@mpi-hd.mpg.de
†Electronic address: s.fritzsche@physik.uni-kassel.de

first to investigate the population of these states as it arises due to the electron capture process. In Sec. II A, we present basic formulas, derived from the density-matrix approach, for the electron capture into many-electron ions. In particular, we show how the magnetic sublevel population of the (excited) ion can be described in terms of reduced statistical tensors. The relation between these tensors (or alignment parameters) and the angular distribution of the subsequent radiative decay is obtained in Sec. II B, again with an emphasis on the many-electron case. Apart from the alignment of the excited ionic states and some geometrical factors, in addition, we show that the angular properties of the characteristic radiation also depend on reduced matrix elements (transition amplitudes) which describe the bound-bound transitions in many-electron ions. In Sec. III, the computation of these matrix elements and of the bound-free transition amplitudes within the framework of the multiconfiguration Dirac-Fock (MCDF) method is briefly outlined. This method is later used for the treatment of the alignment of excited ionic states following the *L*- and *M*-shell REC into initially hydrogenlike U^{91+} and lithium-like U^{89+} uranium projectiles. The results of the (many-electron) calculations are presented in Sec. IV and are compared to predictions from a one-particle model. It is found that interelectronic interactions result in an additional alignment of the residual ion which cannot be explained, not even qualitatively, within a one-electron model. Finally, a brief summary of these results and an outlook are given in Sec. V.

II. THEORY

A. Alignment of the excited ion states following the radiative electron capture

During the last decade, the density-matrix theory has been widely applied in studying the radiative electron capture into heavy, highly charged ions. While most of these studies have been dealt with in the past with the electron recombination into the *bare* projectiles [12–14,18,22,23], today's interest is focused on the capture into high-*Z*, *few-electron* ions. Recently, for example, the density-matrix theory helped us to obtain some preliminary results for the total cross sections as well as the angular distributions of the recombination x-ray photons emitted due to the REC into H-, He-, and Li-like uranium projectiles [19,24]. In the derivation of the total and angle-differential cross sections, it was shown that the REC properties can be traced back to the evaluation of a (reduced) matrix element

$$\mathrm{M}_{if}(pL) = \langle (\alpha_i J_i, \epsilon lj) J \| H_\gamma(pL) \| \alpha_f J_f \rangle \tag{1}$$

which describes the capture of a free electron with kinetic energy ϵ and total angular momentum j under the simultaneous emission of a photon with angular momentum L and parity $(-1)^{L+p}$. In this amplitude, moreover, the ion is supposed to be in the states $|\alpha_i J_i\rangle$ and $|\alpha_f J_f\rangle$ with well-defined total angular momenta $J_{i,f}$ just before and after recombination process. Here, α_i and α_f denote all the additional quantum numbers as needed for a unique specification of the states.

The reduced matrix element (1) represents the central building block from which most of the REC properties can be calculated. Apart from the total and angle-differential recombination cross sections, in particular, this matrix can be utilized in order to investigate the magnetic sublevel population of the residual ion $|\alpha_f J_f\rangle$ following electron capture. In the framework of the density-matrix theory, the resulting sublevel population of the ionic (or atomic) states is described most naturally in terms of the so-called *statistical tensors* $\rho_{kq}(\alpha_f J_f)$ which are constructed as to transform like the spherical harmonics of rank k under a rotation of the coordinates [19,25,26]. Of course, the particular form of the statistical tensors typically depend on the choice of the quantization axis of the overall system (z axis). As discussed previously [12], the choice of this quantization axis and hence the projections above depend both on the particular process under consideration and on the experimental geometry. For instance, to explore the magnetic sublevel population of the residual ion following the electron capture, it is convenient to adopt a quantization axis along the incoming ion momentum. For such a choice of the quantization axis, the statistical tensors of the "final"-state ion $|\alpha_f J_f\rangle$ (where "final" refers to the state after the capture, before the subsequent decay) are given by [19]

$$\begin{aligned}\rho_{k0}(\alpha_f J_f) = \frac{32\pi^3}{2J_i+1} \sum_{Lp} \sum_{JJ'\kappa\kappa'} [l,l',j,j',J,J']^{1/2} \\ \times (-1)^{J_i+L-J_f+J-J'-1/2} \langle l0l'0|k0\rangle \\ \times \begin{Bmatrix} j & j' & k \\ l' & l & 1/2 \end{Bmatrix} \begin{Bmatrix} j & j' & k \\ J' & J & J_i \end{Bmatrix} \\ \times \begin{Bmatrix} J & J' & k \\ J_f & J_f & L \end{Bmatrix} \langle (\alpha_i J_i, \epsilon lj) J \| H_\gamma(pL) \| \alpha_f J_f \rangle \\ \times \langle (\alpha_i J_i, \epsilon l'j') J' \| H_\gamma(pL) \| \alpha_f J_f \rangle^* . \end{aligned} \tag{2}$$

Here, the summation over $(LpJ\kappa)$ includes all allowed combinations of the electric $(p=1)$ and magnetic $(p=0)$ multipoles of the radiation field and the many-electron continua $|(\alpha_i J_i, \epsilon lj)J\rangle$ of the initial ion. In Eq. (2), moreover, κ denotes the Dirac's angular momentum quantum number of a free electron, $\kappa = \pm(j+1/2)$ for $l = j \pm 1/2$ and $[l] = (2l+1)$.

Instead of using the statistical tensors (2), it is often more convenient to describe the sublevel population of the residual ions in terms of the so-called *reduced* statistical tensors [13,25,26]

$$\mathcal{A}_{k0}(\alpha_f J_f) = \frac{\rho_{k0}(\alpha_f J_f)}{\rho_{00}(\alpha_f J_f)}, \tag{3}$$

which are directly related to the cross sections $\sigma^{\mathrm{REC}}_{|J_f M_f\rangle}$ for the population of the different ionic sublevels $|\alpha_f J_f M_f\rangle$ (see Ref. [19]). The reduced statistical tensors (3) are known to obey several properties. For example, the tensor $\mathcal{A}_{k0}(\alpha_f J_f)$ is nonvanishing only if k is even and if it satisfies the condition $k \leqslant 2J_f$ [19,25], which constitutes a phenomenologically important constraint. For the electron recombination into any level with $J_f = 1$ therefore there is only one nonvanishing parameter $\mathcal{A}_{20}$ (apart from $\mathcal{A}_{00} \equiv 1$):

$$\mathcal{A}_{20}(\alpha_f J_f = 1) = \sqrt{2}\frac{\sigma^{\mathrm{REC}}_{|J_f=1M_{J,f}=\pm1\rangle} - \sigma^{\mathrm{REC}}_{|J_f=1M_{J,f}=0\rangle}}{\sigma^{\mathrm{REC}}_{|J_f=1M_{J,f}=0\rangle} + 2\sigma^{\mathrm{REC}}_{|J_f=1M_{J,f}=\pm1\rangle}}. \tag{4}$$

In contrast, there are two nonzero parameters for $J_f=2$:

$$\mathcal{A}_{20}(\alpha_f J_f = 2) = -\sqrt{\frac{10}{7}}\frac{\sigma^{\mathrm{REC}}_{|J_f=2M_{J,f}=0\rangle} + \sigma^{\mathrm{REC}}_{|J_f=2M_{J,f}=\pm1\rangle} - 2\sigma^{\mathrm{REC}}_{|J_f=2M_{J,f}=\pm2\rangle}}{\sigma^{\mathrm{REC}}_{|J_f=2M_{J,f}=0\rangle} + 2\sigma^{\mathrm{REC}}_{|J_f=2M_{J,f}=\pm1\rangle} + 2\sigma^{\mathrm{REC}}_{|J_f=2M_{J,f}=\pm2\rangle}} \tag{5}$$

and

$$\mathcal{A}_{40}(\alpha_f J_f = 2) = \sqrt{\frac{2}{7}}\frac{3\sigma^{\mathrm{REC}}_{|J_f=2M_{J,f}=0\rangle} - 4\sigma^{\mathrm{REC}}_{|J_f=2M_{J,f}=\pm1\rangle} + \sigma^{\mathrm{REC}}_{|J_f=2M_{J,f}=\pm2\rangle}}{\sigma^{\mathrm{REC}}_{|J_f=2M_{J,f}=0\rangle} + 2\sigma^{\mathrm{REC}}_{|J_f=2M_{J,f}=\pm1\rangle} + 2\sigma^{\mathrm{REC}}_{|J_f=2M_{J,f}=\pm2\rangle}}. \tag{6}$$

B. Subsequent radiative decay

Equations (2) and (3) together with the bound-free transition amplitude (1) describe the population of a heavy, highly charged ion following the radiative capture of an electron. Of course, if such electron capture occurs into an excited state $|\alpha_f J_f\rangle$ of the ion, the subsequent decay may lead to the emission of one (or several) photons until the ground state $|\alpha_0 J_0\rangle$ is reached. This subsequent radiative decay is characterized (apart from the well-known energies) by its angular distribution and polarization [13,14]. Both of these properties are closely related to the sublevel occupation of the excited ion states and hence to the reduced statistical tensors $\mathcal{A}_{kq}(\alpha_f J_f)$. For instance, the angular distribution of the characteristic photons, emitted in the $|\alpha_f J_f\rangle \to |\alpha_0 J_0\rangle + \gamma$ radiative decay is given by

$$W^{\mathrm{dec}}(\theta) = \frac{\sigma_0^{\mathrm{dec}}}{4\pi}\Bigg(1 + \sum_{k=2,4,\ldots} f_k^{\mathrm{dec}}(\alpha_f J_f, \alpha_0 J_0) \times \mathcal{A}_{k0}(\alpha_f J_f) P_k(\cos\theta)\Bigg), \tag{7}$$

where σ_0^{dec} is the total decay rate and θ denotes the angle of the photons with respect to the direction of the ion beam (quantization axis). We deduce that apart from the reduced statistical tensors $\mathcal{A}_{k0}(\alpha_f J_f)$, the photon angular distribution also depends on the so-called *anisotropy* parameters $f_k^{\mathrm{dec}}(\alpha_f J_f, \alpha_0 J_0)$. These parameters are independent on the electron capture process and merely reflect the electronic structure of the ion. For many-electron ions and with a full account of the different terms in the expansion of the electron-photon interaction, the anisotropy parameter of kth order is given by

$$f_k^{\mathrm{dec}}(\alpha_f J_f, \alpha_0 J_0) = \frac{\sqrt{2J_f+1}}{2}\sum_{LpL'p'} i^{L'+p'-L-p} \times (-1)^{J_0+J_f+k+1}[L,L']^{1/2}\langle L1L'-1|k0\rangle \times (1+(-1)^{L+p+L'+p'-k})\begin{Bmatrix} L & L' & k \\ J_f & J_f & J_0 \end{Bmatrix} \times \langle \alpha_f J_f||H_\gamma(pL)||\alpha_0 J_0\rangle^* \times \langle \alpha_f J_f||H_\gamma(p'L')||\alpha_0 J_0\rangle \times \Bigg[\sum_{Lp} |\langle \alpha_f J_f||H_\gamma(pL)||\alpha_0 J_0\rangle|^2\Bigg]^{-1}. \tag{8}$$

Here, $\langle \alpha_f J_f||H_\gamma(pL)||\alpha_0 J_0\rangle$ denotes the reduced matrix element for the specified bound-bound electron transition. In fact, this matrix element is similar to the bound-free transition amplitude (1), the only difference being that both (many-electron) wave functions on the left- and right-hand sides of the matrix element represent now bound ionic states.

Equations (7) and (8) represent the most general form of the angular distribution of the characteristic radiation following the electron capture into excited ionic states. They include the summation over all the different multipoles (pL) of the radiation field allowed owing to the parity and angular-momentum selection rules. Often, there is one allowed multipole term which dominates the radiative decay for any given pair of initial and final bound states and, sometimes, only one. In many cases therefore the summation over the multipole components of the radiation field can be restricted to just a single term which leads to a significant simplification of Eqs. (7) and (8). For an electric-dipole allowed $(E1)$ radiation, for example, the angular distribution is given by [25,27]

$$W^{\mathrm{dec}}_{E1}(\theta) = \frac{\sigma_0^{\mathrm{dec}}}{4\pi}\Big[1 + f_2^{\mathrm{dec}}(\alpha_f J_f, \alpha_0 J_0; E1)\mathcal{A}_{20}(\alpha_f J_f) P_2(\cos\theta)\Big], \tag{9}$$

with the anisotropy parameter:

$$f_2^{\mathrm{dec}}(\alpha_f J_f, \alpha_0 J_0; E1) = (-1)^{1+J_f+J_0}\sqrt{\frac{3(2J_f+1)}{2}}\begin{Bmatrix} 1 & 1 & 2 \\ J_f & J_f & J_0 \end{Bmatrix}. \tag{10}$$

The electric dipole approximation (9) and (10) seems to be well justified for the radiative decay of low-Z and medium-Z ions, for which the contributions from the nondipole components of the radiation field are negligible. However, for the high-Z domain a significant change in the photon angular distributions may arise due to higher multipoles and may lead to quite sizeable deviations when compared

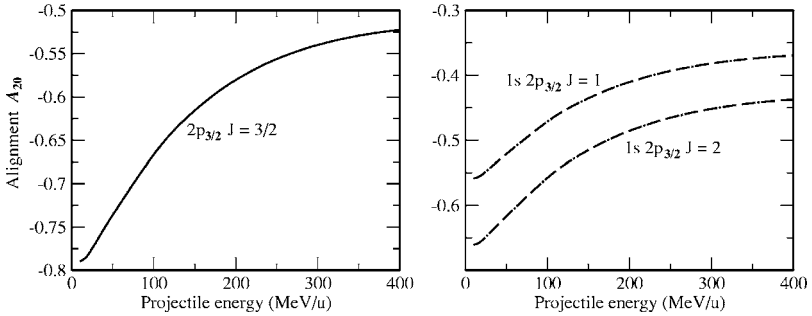

FIG. 1. Alignment parameters $\mathcal{A}_{20}$ of the $2p_{3/2}$ state of hydrogenlike (left panel) and the $1s2p_{3/2}$ $J=1,2$ states of heliumlike (right panel) ions following the radiative electron capture of uranium projectiles. The results of MCDF calculations in Coulomb and Babushkin gauges yield consistent results which are plotted as a single curve.

with the dipole approximation. For example, the multipole mixing between the leading electric dipole ($E1$) and the—much weaker—magnetic quadrupole ($M2$) components of the Lyman-α_1 ($2p_{3/2} \rightarrow 1s_{1/2}$) transition in heavy, hydrogenlike ions is known to modify the anisotropy parameter (10):

$$f_2^{\mathrm{dec}}(2p_{3/2}J_f = 3/2, 1s_{1/2}J_0 = 1/2) \approx \frac{1}{2}\left(1 + 2\sqrt{3}\frac{\langle 2p_{3/2}J_f = 3/2 \| H_\gamma(M2) \| 1s_{1/2}J_0 = 1/2\rangle}{\langle 2p_{3/2}J_f = 3/2 \| H_\gamma(E1) \| 1s_{1/2}J_0 = 1/2\rangle}\right), \tag{11}$$

giving rise to a 20–30 % magnetic quadrupole correction over the dipole approximation [13,14] in the angular distributions. Besides the hydrogen like ions, similar sizable corrections can be expected also for few-electron ions. The analysis of such—nondipole—effects in the radiative decay of the berylliumlike U^{88+} uranium ions will be given at the end of Sec. IV.

III. COMPUTATIONS

As seen from Eqs. (2), (3), (7), and (8), one needs to calculate the reduced matrix elements $\langle (\alpha_i J_i, \epsilon lj) J \| H_\gamma(pL) \| \alpha_f J_f \rangle$ and $\langle \alpha_f J_f \| H_\gamma(pL) \| \alpha_0 J_0 \rangle$ for any further analysis of both the statistical tensors of the excited ion states as well as the angular distribution of the characteristic radiation, respectively. These matrix elements frequently occur in the computation of the different atomic properties [19,24,28,29] and have been implemented in quite a number of calculational approaches. In the computations below, for instance, the alignment parameters of the residual ion have been calculated by means of the multiconfiguration Dirac-Fock (MCDF) method. In this method, both the initial and the final ionic states with angular momentum J and parity P are approximated by a linear combination of (so-called) configuration state functions (CSFs) of the same symmetry:

$$\psi_\alpha(PJM) = \sum_{r=1}^{n_c} c_r(\alpha) | \gamma_r PJM \rangle, \tag{12}$$

where n_c is the number of CSFs and $\{c_r(\alpha)\}$ denotes the representation of the atomic state in this basis. As usual, the CSFs are antisymmetrized products of a common set of orthonormal orbitals which are optimized together on the basis of the Dirac-Coulomb Hamiltonian. Further relativistic contributions to the decomposition $\{c_r(\alpha)\}$ of the atomic states are then added, owing to the given requirements, by rediagonalizing the Dirac-Coulomb-Breit Hamiltonian matrix. Quantum electrodynamic corrections are beyond the level of accuracy of the angular resolution in the experiments which we aim to describe with our calculations.

In order to support a reliable estimate of the REC matrix elements, a different component (REC) has been developed recently within the framework of the RATIP package [30] which now facilitates the computation of total and angle-differential cross sections as well as alignment parameters in a distorted-wave approximation.

IV. RESULTS AND DISCUSSION

As discussed recently [19,24], the REC into high-Z, few-electron ions may serve as a valuable tool for studying the interplay between the electron-photon and electron-electron interactions in the presence of strong electromagnetic fields, produced by heavy nuclei. In practice, however, the total and angle-differential REC cross sections are rather insensitive to the interelectronic interaction effects. In contrast to the recombination x-ray photons, one may expect that the analysis of the characteristic radiation, if possible, may provide more information on the electron-electron repulsion. As shown in Sec. II B, however, the properties of this characteristic radiation are closely related to the magnetic sublevel population of the excited ionic (or atomic) states which is described in terms of the so-called alignment parameters. Below therefore we apply Eqs. (2) and (3) to study the alignment of the excited, few-electron ions following the electron recombination process. In the current theoretical study, we focus on the capture into initially hydrogen U^{91+} and lithiumlike U^{89+} uranium projectiles (as the simplest examples of many-electron, high-Z systems), for which the fine structure of the ions is expected to influence the alignment of their excited states.

For hydrogenlike ions, experiments have been performed recently at the GSI storage ring [20,21] in order to explore the electron capture into the $2p_{3/2}$ subshell, leading to the $1s2p_{3/2}\,{}^{1,3}P_{J=1,2}$ states of (finally) heliumlike system. The special interest to the alignment analysis of these excited states arises from the fact that the REC into the *bare* projectiles is known to produce the strong alignment of the $2p_{3/2}\,{}^2P_{j=3/2}$ level of the residual (hydrogenlike) ions [14,23,31]. As seen from the left panel of Fig. 1, the alignment of the $2p_{3/2}$ state following REC of bare uranium ions U^{92+} is almost $\mathcal{A}_{20}=-0.8$ at the projectile energy $T_p = 10$ MeV/u and slightly decreases to $\mathcal{A}_{20}=-0.523$ for higher energies. Since, however, the two-electron states

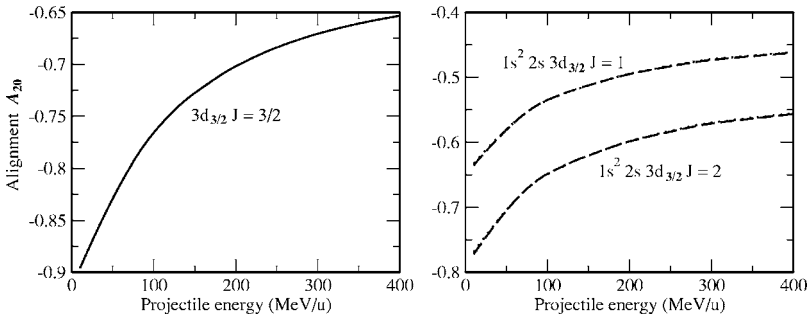

FIG. 2. Alignment parameters $\mathcal{A}_{20}$ of the $3d_{3/2}$ state of hydrogenlike (left panel) and the $1s^2 2s 3d_{3/2}$ $J=1,2$, states of berylliumlike (right panel) ions following the radiative electron capture into uranium projectiles. Again, the results of MCDF calculations in Coulomb and Babushkin gauges yield consistent results which are plotted as a single curve.

$1s2p_{3/2}\ ^{1,3}P_{J=1,2}$ differ from the hydrogenlike system only by the coupling of the electron angular momenta and, for high-Z ions, some interelectronic effects, one also expects a nonvanishing alignment of the heliumlike uranium ions U^{90+} following the capture into a $2p_{3/2}$ subshell. In this contribution, we make use of Eqs. (2) and (3) to investigate the reduced statistical tensors $\mathcal{A}_{20}$ of the $1s2p_{3/2}\ ^{1,3}P_{J=1,2}$ levels following the REC into initially hydrogenlike projectiles. Calculations were performed within the MCDF approximation in which two different gauges (Babushkin and Coulomb) have been adopted for the coupling of the radiation field. For the capture into hydrogenlike uranium U^{91+}, these gauges yield basically identical results (with a deviation of less than 0.3%), as displayed in the right panel of Fig. 1. As seen from this figure, both $1s2p_{3/2}$ $J=1,2$ levels appear to be strongly aligned in the course of the REC process. The alignment of these states behaves rather similarly to the alignment of the one-electron system (cf. the left panel of Fig. 1), but differs from the one-electron case by almost constant factors of about 1.42 and 1.20 for $J=1$ and $J=2$, respectively, over the entire range of projectile energies considered here. Similar to the recombination of bare ions, furthermore, the reduced statistical tensors $\mathcal{A}_{20}(J=1)$ and $\mathcal{A}_{20}(J=2)$ are negative for the energies $10 \leqslant T_p \leqslant 400$ MeV/u, referring to a predominant population of the $M_J=0$ magnetic substate [cf. Eqs. (4) and (5)] and hence to an alignment which could be characterized as *perpendicular* to the beam direction. This interpretation is consistent with a classical picture, in which the orbital angular momentum transferred in a collision is found perpendicular to the collision plane [23].

Apart from the alignment parameter $\mathcal{A}_{20}$, the magnetic sublevel population of the $1s2p_{3/2}$ $J=2$ state also entails the reduced statistical tensor $\mathcal{A}_{40}$ [cf. Eqs. (5) and (6)]. From our MCDF calculations, however, we found that this parameter does not exceed a value of 10^{-4} for the projectile energies in the range $10 \leqslant T_p \leqslant 400$ MeV/u. The rather small alignment $\mathcal{A}_{40}$ of the heliumlike system again illustrates the similarity to the electron capture into the $2p_{3/2}$ state of initially bare ions for which the statistical tensor of fourth rank identically vanishes.

Until now, we have discussed the electron recombination into the $1s2p_{3/2}\ ^{1,3}P_{J=1,2}$ levels of initially hydrogenlike ions. The alignment of these levels was found to exhibit quite a similar behavior as compared to the alignment of the $2p_{3/2}$ state following the REC into bare projectiles. In order to obtain a more complete picture of the electron-electron contributions to the magnetic sublevel population of the excited ionic states, one may consider also the capture into initially lithiumlike ions. This is known to be more sensitive to many-particle effects [19]. For initially lithiumlike ions therefore we explore the M-REC into the $1s^2 2s3lj\ ^{1,3}L_J$ levels (of finally berylliumlike projectiles). As for the L-shell capture, let us start the analysis of the alignment of these states by considering first the M-REC into bare projectiles. The alignment of the $3p_{3/2}$, $3d_{3/2}$, and $3d_{5/2}$ states of (finally) hydrogenlike ions have been studied previously by Eichler and co-workers [23] for a wide range of projectile energies. Special attention in these studies has been paid to the d levels which can decay into the $1s_{1/2}$ ground state by a (leading) electric quadrupole transition. For the electron recombination into the $3d_{3/2}$ state, e.g., the $\mathcal{A}_{20}$ parameter was found to change from about -0.9 to -0.65 in the energy region $10 \leqslant T_p \leqslant 400$ MeV/u (cf. the left panel of Fig. 2). In order to explore the behavior of this parameter for few-electron systems, we have calculated the REC into the $1s^2 2s_{1/2} 3d_{3/2}\ ^3D_{J=1,2}$ states of initially lithiumlike uranium ions. As seen from the right panel of Fig. 2, a strong negative alignment arises for both $J=1,2$ levels, corresponding (again) to a preferred population of the $M_J=0$ magnetic substate. Similar to the U^{90+} case, moreover, the alignment of these many-electron states is weaker by approximate factors of 1.41 (for $J=1$) and 1.16 (for $J=2$) as compared to the corresponding alignment of one-electron system, over the entire range of projectile energies.

In Fig. 2, we display the energy dependence of the reduced statistical tensor $\mathcal{A}_{20}$ following REC into the $3d_{3/2}$ state of bare as well as lithiumlike uranium ions. While this second-rank tensor contains the complete information on the magnetic sublevel population of the (finally) hydrogenlike ions, one additionally needs also the fourth-rank tensor element $\mathcal{A}_{40}$ in order to describe the alignment of few-electron ions with $J=2$. For the capture into the $1s^2\ 2s_{1/2} 3d_{3/2}\ ^3D_{J=2}$ state of the (finally) berylliumlike uranium ions U^{88+}, for instance, the statistical tensor $\mathcal{A}_{40}$ appears to be positive for all projectile energies in the range $10 \leqslant T_p \leqslant 400$ MeV/u (cf. Fig. 3). Such a—nonvanishing—tensor may arise mainly due to the mixture of the $1s^2 2s_{1/2} 3d_{5/2}\ ^3D_{J=2}$ level with other levels having a strong alignment. From our MCDF calculations, in particular, we found an admixture of about 0.2% of the $1s^2 2s_{1/2} 3d_{5/2}\ ^1D_{J=2}$ level for which a large positive parameter $\mathcal{A}_{40}$ has been obtained both within the "one-electron" [23] as well as the MCDF calculations. These results are shown in the bottom panels of Fig. 4. As seen from this figure, moreover, a good agreement is found for the $\mathcal{A}_{40}$ parameter between the Coulomb and Babushkin gauge for the coupling of the radiation field to the electron density. This agreement

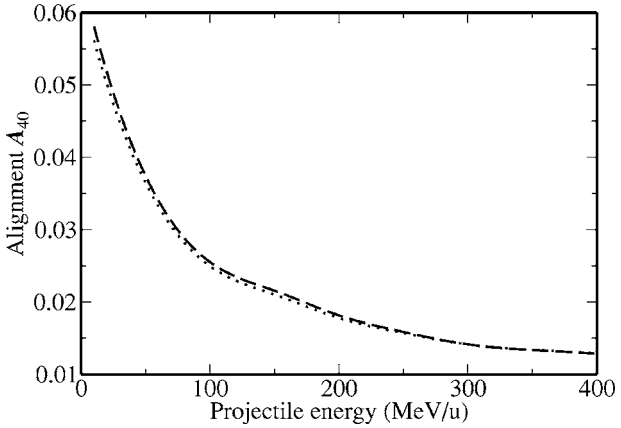

FIG. 3. Alignment parameter $\mathcal{A}_{40}$ of the $1s^2 2s_{1/2} 3d_{3/2}\ ^3D_{J=2}$ state following the radiative electron capture of (initially) lithiumlike uranium ions U^{89+} (finally berylliumlike). For the corresponding capture into the $3d_{3/2}$ state of initially bare uranium, the alignment parameter $\mathcal{A}_{40}$ identically vanishes. Results from MCDF calculations are shown in Coulomb (dotted line) and Babushkin gauges (dashed line).

indicates that even a rather restricted wave-function expansion is sufficient for high-Z ions, such as U^{88+}, in order to describe most properties accurately (cf. Fig. 3 also). Although an agreement of the theoretical predictions from different gauges cannot "prove" the correctness of the results, their deviations are often taken as a first sign for the quality of the many-electron computations.

As seen from Eq. (7), the nonzero alignment $\mathcal{A}_{40}$ may modify the angular distribution of the subsequent radiative decay which contains the Legendre polynomials $P_k(\cos\theta)$ as well as the anisotropy parameters $f_k^{\rm dec}(\alpha_f J_f, \alpha_0 J_0)$ of the second and the fourth order. However, since the anisotropy parameter (8) should obey the triangle rule $0 \leqslant k \leqslant 2L$, where L is the angular momentum of the decay photons, the fourth-rank statistical tensor $\mathcal{A}_{40}$ does not affect the emission of the dipole radiation ($L=1$). The contribution from this tensor can be observed therefore only for the bound-bound transitions for which, apart from the leading dipole term, also higher multipoles of the radiation field become allowed. In order to investigate such nondipole effects as well as the contribution from the nonzero alignment parameter $\mathcal{A}_{40}$, we display in Fig. 5 the angular distribution of the $1s^2 2s_{1/2} 3d_{3/2}\ ^3D_{J=2} \rightarrow 1s^2 2s_{1/2} 2p_{3/2}\ ^1P_{J=1}$ decay following REC into (initially) lithiumlike ions with energies $T_p = 10$, 200, and 400 MeV/u. Calculations have been performed within the electric dipole approximation (dashed line), which is given by Eqs. (9) and (10), as well as within the "exact" relativistic treatment (solid line). Apart from the—leading—electric dipole (*E1*) transition, the exact treatment takes into account both, the magnetic quadrupole (*M2*) and electric octupole (*E3*) decay channels. These higher multipoles not only modify the second-order anisotropy parameter (10) but give also rise to a nonzero parameter $f_4^{\rm dec}(\alpha_f J_f, \alpha_0 J_0)$ which is weighted by the alignment $\mathcal{A}_{40}$ [cf. Eq. (7)]. As seen from Fig. 5, however, the nondipole terms result in a relatively small deviation of the angular distribution of the $^3D_2 \rightarrow {}^1P_1$ radiation when compared with the electric dipole approximation. In fact, such a small correction can hardly be measured in present-day experiments due to the resolution limitations of detectors for hard x rays. Therefore other bound-bound transitions have to be considered in order to explore the nondipole effects in berylliumlike ions. Figure 6, for example, shows how the multipole mixing between the magnetic dipole (*M1*), electric quadrupole (*E2*), as well magnetic octupole (*M3*) decay channels strongly modifies the angular distribution of the $1s^2 2s_{1/2} 3d_{3/2}\ ^3D_{J=2} \rightarrow 1s^2 2s_{1/2} 3s_{1/2}\ ^3S_{J=1}$ radiative decay and hence may allow us to measure the (additional) alignment $\mathcal{A}_{40}$ of the $^3D_2$ level.

Of course, apart from the $1s^2 2s_{1/2} 3d_{3/2}\ ^3D_{J=2}$ level, one can expect that the corresponding admixtures will lead to an additional alignment also for the other excited states of berylliumlike ion. For instance, a nonzero alignment $\mathcal{A}_{20}$ was found for the electron capture into the $1s^2 2s_{1/2} 3s_{1/2}\ ^3S_{J=1}$ state due to the admixture of the (strongly aligned) $1s^2 2s_{1/2} 3d_{3/2}\ ^3D_{J=1}$ level. However, since the mixing coefficient for the $1s^2 2s_{1/2} 3d_{3/2}\ ^3D_{J=1}$ level appears to be only $5 \times 10^{-4}\%$, the second-rank tensor $\mathcal{A}_{20}$ does not exceed 10^{-5} for the collision energies $10 \leqslant T_p \leqslant 400$ MeV/u which is much below the present-day experimental accuracy. Therefore in order to explore the many-electron contributions to the alignment of the residual ions, one has to consider the

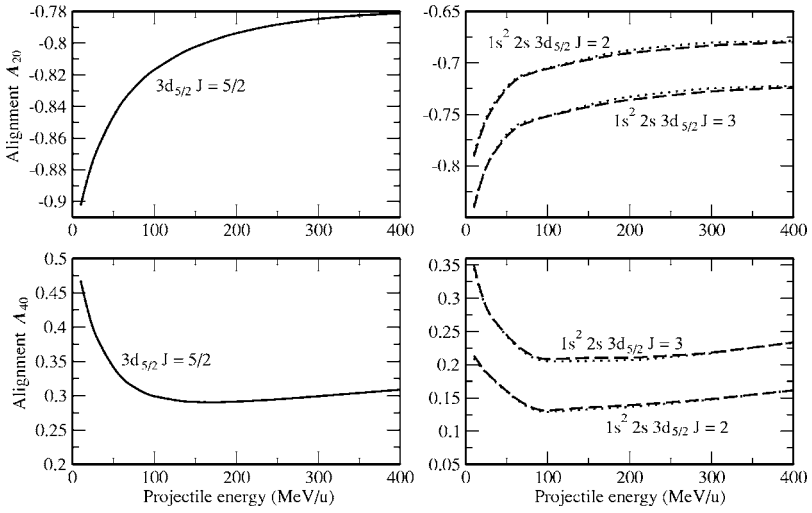

FIG. 4. Alignment parameters $\mathcal{A}_{20}$ and $\mathcal{A}_{40}$ of the $3d_{5/2}$ state of hydrogenlike (left panels) and the $1s^2 2s_{1/2} 3d_{5/2}\ ^{1,3}D_{J=2,3}$ states of berylliumlike (right panels) ions following the radiative electron capture into uranium projectiles. Results from MCDF calculations are shown in Coulomb (dotted line) and Babushkin gauges (dashed line).

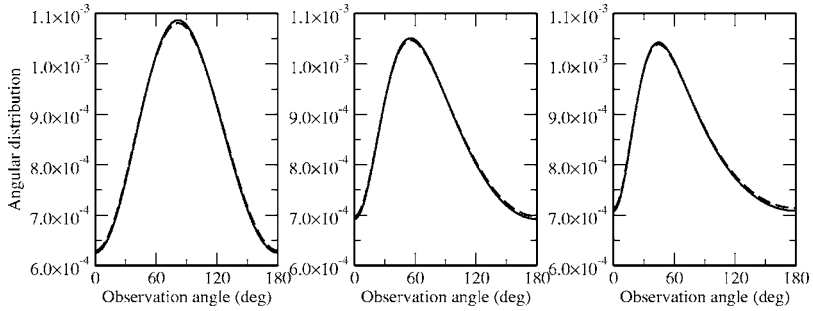

FIG. 5. Angular distribution of the $1s^2 2s_{1/2} 3d_{3/2}\ ^3D_{J=2} \rightarrow 1s^2 2s_{1/2} 2p_{3/2}\ ^1P_{J=1}$ decay following REC into the (initially) lithiumlike projectile ions with energies $T_p = 10$ MeV/u (left panel), $T_p = 200$ MeV/u (middle panel), and $T_p = 400$ MeV/u (right panel). Results are presented within the laboratory frame for the exact relativistic theory (solid line) and the electric dipole approximation (dashed line). Following the experimental technique applied in Ref. [21], the angular distribution is normalized to the intensity of the isotropic Lyman-α_2 radiation in hydrogen like U^{91+} ions.

electron recombination either into the d levels or for the medium-Z ions, for which a stronger configuration mixing between the ^3S and ^3D levels occurs.

V. SUMMARY AND OUTLOOK

In this paper, the radiative electron capture into excited states of highly charged, few-electron ions has been studied within the framework of the density-matrix theory and combined with multiconfiguration Dirac-Fock computations. From the density matrix of the initial ion "plus" free (or quasifree) electron, we derived the general expressions for the alignment parameters $\mathcal{A}_{k0}$ which can be employed to describe the magnetic sublevel population of the residual ion. These expressions neither depend on the number of electrons nor on the shell structure of the ions, but detailed computations have been carried out only for the recombination of initially hydrogenlike and lithiumlike uranium projectiles. For these ions, the magnetic sublevel population of (most of) the excited states exhibits a behavior similar to the alignment of the corresponding one-electron levels as it arises from the REC into initially bare projectiles. In some cases, however, the many-electron effects result in an additional alignment of the residual ions which cannot be predicted (even qualitatively) from the "one-electron" calculations. For the electron capture into the $1s^2 2s_{1/2} 3d_{3/2}\ ^3D_{J=2}$ state of lithiumlike uranium ions, for example, the admixture of the $1s^2 2s_{1/2} 3d_{5/2}\ ^1D_{J=2}$ configuration gives rise to a nonvanishing fourth-rank parameter $\mathcal{A}_{40}$ which is otherwise identical to zero for the $3d_{3/2}\ ^2D_{J=3/2}$ level of one-electron system.

In contrast to the total REC cross sections and the angular distributions of the recombination photons, the magnetic sublevel population of the residual ion cannot be measured directly in any experiment. Instead, this sublevel population is usually derived from the measuring the subsequent radiative decay of the ion when an electron is initially captured into an excited state. In Sec. II B therefore we derive the general expressions for the angular distribution of the characteristic radiation which take into account the alignment of the excited states as well as the electronic structure of the ion. These expressions are applied in Sec. IV in order to discuss the many-electron as well as the nondipole effects in the radiative decay of the $1s^2 2s_{1/2} 3d_{3/2}\ ^3D_{J=2}$ state of beryllliumlike U^{88+} uranium ions following REC process. While the calculations for the berylliumlike projectiles are performed mainly in illustration purposes, in the future we intent to utilize our formalism for analyzing the available experimental data on the x-ray emission from the heavy, few-electron ions. In particular, we currently investigate the electron capture into the $1s2p_{1/2}$ and $1s2p_{3/2}\ ^{1,3}P_{J=1,2}$ levels of initially hydrogenlike uranium ions and their subsequent

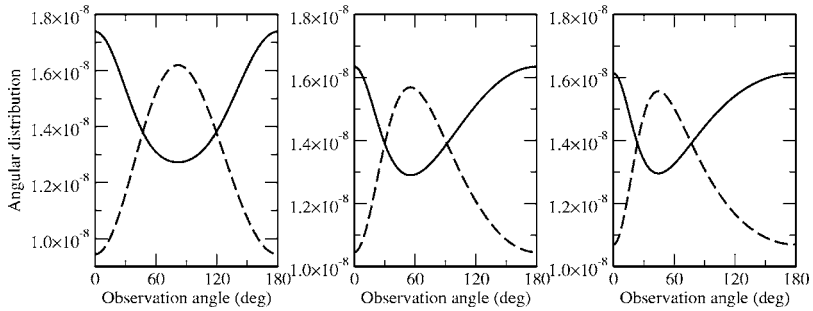

FIG. 6. Angular distribution of the $1s^2 2s_{1/2} 3d_{3/2}\ ^3D_{J=2} \rightarrow 1s^2 2s_{1/2} 3s_{1/2}\ ^3S_{J=1}$ decay following REC into the (initially) lithiumlike projectile ions with energies $T_p = 10$ MeV/u (left panel), $T_p = 200$ MeV/u (middle panel), and $T_p = 400$ MeV/u (right panel). Results are presented within the laboratory frame for the exact relativistic theory (solid line) and the magnetic dipole approximation (dashed line). Following the experimental technique applied in Ref. [21], the angular distribution is normalized to the intensity of the isotropic Lyman-α_2 radiation in hydrogenlike U^{91+} ions.

$K\alpha_1$ and $K\alpha_2$ decay (the $J=0$ states cannot be aligned). Experiments concerning these states have recently been performed at the ESR storage ring at GSI, and the angular distributions observed [20,21] have been found to be inconsistent with the predictions of a one-particle model.

ACKNOWLEDGMENTS

U.D.J. acknowledges support by the Deutsche Forschungsgemeinschaft (Heisenberg program). S.F. acknowledges support by the BMBF and the GSI under Project No. KS-FRT.

[1] H. F. Krause, C. R. Vane, S. Datz, P. Grafström, H. Knudsen, C. Scheidenberger, and R. H. Schuch, Phys. Rev. Lett. **80**, 1190 (1998).
[2] Th. Stöhlker, Phys. Scr. **T80**, 165 (1999).
[3] Th. Stöhlker, X. Ma, T. Ludziejewski, H. F. Beyer, F. Bosch, O. Brinzanescu, R. W. Dunford, J. Eichler, S. Hagmann, A. Ichihara, C. Kozhuharov, A. Krämer, D. Liesen, P. H. Mokler, Z. Stachura, P. Swiat, and A. Warczak, Phys. Rev. Lett. **86**, 983 (2001).
[4] Th. Stöhlker, D. Banas, S. Fritzsche, A. Gumberidze, C. Kozhuharov, X. Ma, A. Orsic-Muthig, U. Spillmann, D. Sierpowski, A. Surzhykov, S. Tachenov, and A. Warczak, Phys. Scr. **T110**, 384 (2004).
[5] G. Bednarz, A. Warczak, D. Sierpowski, Th. Stöhlker, S. Hagmann, F. Bosch, A. Gumberidze, C. Kozhuharov, D. Liesen, P. H. Mokler, X. Ma, and Z. Stachura, Hyperfine Interact. **146/147**, 29 (2003).
[6] R. E. Marrs, P. Beiersdorfer, and D. Schneider, Phys. Today **47** (652), 27 (1994).
[7] P. Beiersdorfer, B. Beck, J. A. Becker, J. K. Lepson, and K. J. Reed, in *X-Ray and Inner-Shell Processes*, edited by A. Marcelli, A. Bianconi, and N. L. Saini, AIP Conf. Proc. No. 652 (AIP, Melville, NY, 2003).
[8] R. H. Pratt, A. Ron, and H. K. Tseng, Rev. Mod. Phys. **45**, 273 (1973).
[9] J. H. Scofield, Phys. Rev. A **40**, 3054 (1989).
[10] J. H. Scofield, Phys. Rev. A **44**, 139 (1991).
[11] J. Eichler and W. Meyerhof, *Relativistic Atomic Collisions* (Academic Press, San Diego, 1995).
[12] A. Surzhykov, S. Fritzsche, and Th. Stöhlker, Phys. Lett. A **289**, 213 (2001).
[13] A. Surzhykov, S. Fritzsche, and Th. Stöhlker, J. Phys. B **35**, 3713 (2002).
[14] A. Surzhykov, S. Fritzsche, A. Gumberidze, and Th. Stöhlker, Phys. Rev. Lett. **88**, 153001 (2002).
[15] S. Fritzsche, A. Surzhykov, and Th. Stöhlker, Nucl. Instrum. Methods Phys. Res. B **205**, 469 (2003).
[16] A. B. Voitkiv, Phys. Rep. **392**, 191 (2004).
[17] S. Fritzsche, P. Indelicato, and Th. Stöhlker, J. Phys. B **38**, S707 (2005).
[18] A. Surzhykov, S. Fritzsche, Th. Stöhlker, and S. Tachenov, Phys. Rev. A **68**, 022710 (2003).
[19] S. Fritzsche, A. Surzhykov, and Th. Stöhlker, Phys. Rev. A **72**, 012704 (2005).
[20] X. Ma, P. H. Mokler, F. Bosch, A. Gumberidze, C. Kozhuharov, D. Liesen, D. Sierpowski, Z. Stachura, Th. Stöhlker, and A. Warczak, Phys. Rev. A **68**, 042712 (2003).
[21] A. Gumberidze, Th. Stöhlker, G. Bednarz, F. Bosch, S. Fritzsche, S. Hagmann, D. C. Ionescu, O. Klepper, C. Kozhuharov, A. Krämer, D. Liesen, X. Ma, R. Mann, P. H. Mokler, D. Sierpowski, Z. Stachura, M. Steck, S. Toleikis, and A. Warczak, Hyperfine Interact. **146/147**, 133 (2003).
[22] J. Eichler, Nucl. Phys. A **572**, 147 (1994).
[23] J. Eichler, A. Ichihara, and T. Shirai, Phys. Rev. A **58**, 2128 (1998).
[24] S. Fritzsche, A. Surzhykov, and G. Gaigalas (unpublished).
[25] E. G. Berezhko and N. M. Kabachnik, J. Phys. B **10**, 2467 (1977).
[26] K. Blum, *Density Matrix Theory and Applications* (Plenum, New York, 1981).
[27] V. V. Balashov, A. N. Grum-Grzhimailo, and N. M. Kabachnik, *Polarization and Correlation Phenomena in Atomic Collisions* (Kluwer Academic Plenum Publishers, New York, 2000).
[28] I. P. Grant, Adv. Phys. **19**, 747 (1970).
[29] I. P. Grant, J. Phys. B **7**, 1458 (1974).
[30] S. Fritzsche, J. Electron Spectrosc. Relat. Phenom. **114-16**, 1155 (2001).
[31] Th. Stöhlker, F. Bosch, A. Gallus, C. Kozhuharov, G. Menzel, P. H. Mokler, H. T. Prinz, J. Eichler, A. Ichihara, T. Shirai, R. W. Dunford, T. Ludziejewski, P. Rymuza, Z. Stachura, P. Swiat, and A. Warczak, Phys. Rev. Lett. **79**, 3270 (1997).